Materials Today: Proceedings 57 (2022) 607–614

Contents lists available at ScienceDirect

Materials Today: Proceedings

journal homepage: www.elsevier.com/locate/matpr

Experimental and modelling of temperature-dependent mechanical properties of CNT/polymer nanocomposites

S. Tamayo-Vegas [a,*], K. Lafdi [a,b]

[a] Northumbria University, Newcastle upon Tyne NE7 7YT, United Kingdom
[b] University of Dayton, OH 45469, United States

ARTICLE INFO

Article history:
Available online 11 February 2022

Keywords:
Polymer-matrix composites (PMCs)
Dynamic mechanical thermal analysis
Micromechanics
Finite element analysis
Thermomechanical modelling
Carbon nanotubes

ABSTRACT

Polymer-matrix composites (PMC) reinforced with nanofillers are in constant demand in various industrial applications. Among nano reinforcements, carbon nanotubes (CNT), show a unique combination of physical properties. Often, PMC/CNT composites perform under harsh operating and environmental conditions ranging from aggressive chemical attacks to high temperatures. Material characterization is critical for correct implementation in multifunctional systems. In this study, we have developed two Representative Volume Elements based on the formation of agglomeration above 2 wt% percentage of CNTs. Using finite element analysis (FEA) we studied the mechanical properties of the nanocomposites as a function of temperature. The viscoelastic properties of different percentages of nanofillers (i.e., 0.5, 1, 2, 4, 5 wt%) were derived. Experimental validation was performed with the samples containing the percentages of nanofillers. The samples were tested using Dynamic Mechanical Analysis (DMA) equipment employing the three-point bending method at a fixed frequency. The data shows that the nanofillers drastically influenced the storage, loss modulus and loss factor with a small addition of carbon nanotubes. The viscoelastic properties are presented from temperatures ranging from 40 ℃ to 120 ℃. Finally, a good agreement between the numerical and experimental approaches was found.

1. Introduction

Since the discovery of carbon nanotubes (CNTs) in 1991 by the scientist Iijima [1], and their first use in polymer composites in 1994 [2], carbon nanotubes, have attracted a large number of research interests in academia and industry [3–7]. Their remarkable combination of mechanical, electrical and thermal properties [8–10] along with excellent physical properties such as large aspect ratio [11], flexibility, low mass density [12], high strength and stiffness [13] make CNTs ideal reinforcement candidates for polymeric nanocomposites. Among polymeric matrices, epoxy resins are the most common thermosetting resin employed for tailoring multifunctional nanocomposites due to their intrinsic high tensile strength, stiffness, reasonable chemical and corrosion resistance and high adhesion to the embedded fillers [4,9,14,15].

These high-performance nanocomposites have diversified applications i.e. construction, aerospace, medical, and electronics [16,17]. Generally, they are exposed to harsh operating and environmental conditions ranging from aggressive chemical attacks to high temperatures [18]. Therefore, from the development point of view characterizing the nanocomposites is a critical task for a coherent design of multifunctional systems. For this matter, several types of research (i.e. theoretical, experimental, and numerical) works have been performed to evaluate the final properties of the nanocomposites and their interaction with the systems [4,19]. Extensive studies have proved the ability of CNTs to improve the electrical [20–24], mechanical [25–29], and thermal properties [30–34]. The electrical and thermal properties follow a phenomenon called the percolation threshold, where the maximum conductivities are attained [20]. Mechanical studies have mostly concentrated on the enhancement in the mechanical properties (i.e. tensile, young's modulus, shear, etc.). Theoretically, with the addition of CNTs the mechanical properties of the matrix are enhanced, however, some experimental studies have shown an adverse effect on the final properties. This phenomenon is mainly attributed to the formation of agglomerates and poor interphase properties.

* Corresponding author.

https://doi.org/10.1016/j.matpr.2022.01.480

In the same manner, the viscoelasticity behavior of the composite seems to be affected. In the literature, there are limited studies regarding the viscoelasticity properties. The studies [35–40] have investigated the influences of CNTs in the final viscoelastic properties. For instance, [41] investigated the storage and loss moduli of various nanocomposites containing carbon nanotubes. The viscoelastic properties were investigated at various frequencies. A simple model was built to predict storage and loss moduli. The model was found to predict the experimental data at the various frequency ranges. Similarly, [42] developed a temperature-dependent model to describe the storage modulus of epoxy composites. [43] generated a semi-analytical model to predict the behavior of the relaxation properties employing a representative unit cell using finite element analysis. The model is capable to describe the viscoelastic properties of polymer composites.

From this brief literature review, it can be said that the majority of researchers studied the viscoelasticity properties of the nanocomposite with a frequency domain approach. Temperature-dependent approaches are not widely studied and understood. Thus, in this study, we have explored the viscoelasticity properties (i.e. storage modulus, loss modulus and loss factor) as a function of temperature. We have developed an RVE model based on finite element analysis (FEA) to predict the behavior of epoxy/CNT nanocomposites. Five models containing 0.5, 1, 2, 4, and 5 wt% of multiwalled carbon nanotubes (MWCNT) in an epoxy matrix were simulated using DIGIMAT FE software. Experimental validation was conducted employing Dynamic Mechanical Analysis equipment. A three-bending point (TBP) method was utilized to characterize the pristine epoxy at a fixed frequency of 1 Hz from temperatures from 40C to 175C. The same approach was utilized on the composite samples. The storage, loss modulus and loss factor were obtained. The numerical modelling data were compared with the experimental storage results resulting in a good agreement.

2. Materials and experimental methods.

2.1. Materials and samples preparation

In this study, laminate samples consisting of neat Epoxy and composite samples of Epoxy matrix reinforced with carbon nanotubes were considered. The matrix was a commercial Epoxy EPON 862. The nanofillers were multi-walled carbon nanotubes (MWCNT) purchased from Applied sciences Inc. MWCNT dimensions range from 100 nm to 200 nm and 30 μm to 100 μm for diameter and length respectively. The samples were fabricated containing different percentages of MWCNT i.e. 0.5, 1, 2, 4, 5 wt %. The samples were tested under thermo-mechanical analysis.

2.2. Dynamic mechanical analysis

The thermo-mechanical analysis was performed with a dynamic mechanic analyser (DMA) TA Instruments Q800. Cantilever three-point bending (TPB) mode at a fixed frequency of 1 Hz was utilised Fig. 3. The neat Epoxy sample with dimensions of 1 mm (length) × 0.0465 mm (width) × 20 mm (thickness) was exposed to a ramp temperature method ranging from 40 °C to 175 °C with an increment of 5 °C/min. The samples containing MWCNT with the same dimensions as the neat sample was exposed to a ramp temperature method ranging from 40 °C to 120 °C with an increment of 5 °C/min. The storage, loss modulus and loss factor as a function of temperature were measured.

2.3. FE simulation of nanocomposite

The nanocomposite simulation was performed in the software DIGIMAT-FE. The micromechanical model involved a three-dimensional representative volume element (RVE). The two-phase RVEs containing Epoxy and randomly distributed MWCNT of different percentages are shown in Fig. 1. The mechanical properties of the constituents are summarized in Table 1 [44,45].

RVE dimensions were set to 20 μm (length) × 20 μm (width) × 20 μm (thickness). The nanofillers were considered as straight cylindrical shapes. Random generation of CNT was performed with dimensions of 150 nm for the diameter and length within the limits of 30 μm to 100 μm respectively. Penetration of nanofillers was allowed. Two different RVE approaches were utilized as shown in Fig. 2. Above 2 wt% the RVE showed in Fig. 2 b) was investigated. The experimental data obtained from the TBP of the pristine epoxy of storage modulus as a function of temperature was utilized to obtain the series function of temperature dependency of the matrix phase in DIGIMAT-FE. The function was utilized for all the models and the behavior of the fillers was obtained through the finite element simulations.

3. Results and discussions.

3.1. Effect of MWCNT on the viscoelastic properties

Fig. 4 depicts the experimental results of storage modulus (E'), loss modulus (E'') and loss factor (Tan) of the pristine epoxy resin and epoxy/CNT composites with the percentages of 0.5, 1 and 2 wt% plotted against temperature. The samples of the pristine epoxy and nanocomposites show a glass state at temperatures below 65 °C and a rubber state at temperatures above 75° C. The data suggests that the glass transition regions occurs between the temperatures of 65 to 75 °C. However, for the sample containing 0.5 wt% of MWCNT, the transition seems to be more abrupt, taking place between 63 and 65 °C. This can be due to the small percentage of nanofillers and the intrinsic properties of the matrix.

The Fig. 4 a) depicts the storage modulus (E') of the samples within temperatures 40 °C to 115 °C. The highest E' value is seen in the region of 40 °C to 60 °C, which determines the glass state region of the samples. The pristine epoxy sample shows a maximum value of 7000 MPa across the glass state temperatures, then the transition to the rubber state takes place in a very narrow temperature region. This phenomenon is seen for the samples containing 0.5 wt%, 1 wt% and 2 wt%. The former adversely showed a decrement in the maximum attainable storage modulus in the glass state compared with the neat epoxy sample. This is seen through the temperature region in the transition state and rubber state. On the other hand, the composites 1 wt% and 2 wt% showed a significant effect on the attainable properties. For instance, the sample containing 1 wt% of MWCNT presented higher values than the neat epoxy in the glass state and is consistent throughout the region temperatures. At lower temperature 40C the maximum storage is attained for Pristine epoxy, the opposite is presented at higher temperatures the maximum storage is for 2% CNT. This phenomenon is presented as at higher temperatures the physical properties of the CNT benefits the rather poor properties of the polymer matrix. The effect is not seeing at high temperatures which one possible reason is the low percentage of CNT.

The transition state seems to follow a close path with the neat epoxy. The rubber state starts within the same temperature regions, however, the storage values for the rubber state are higher and constant at 700 MPa. Furthermore, the sample containing 2 wt % of MWCNT showed a slightly higher value just at the beginning of the glass state. Then the transition takes place at 5 °C degrees

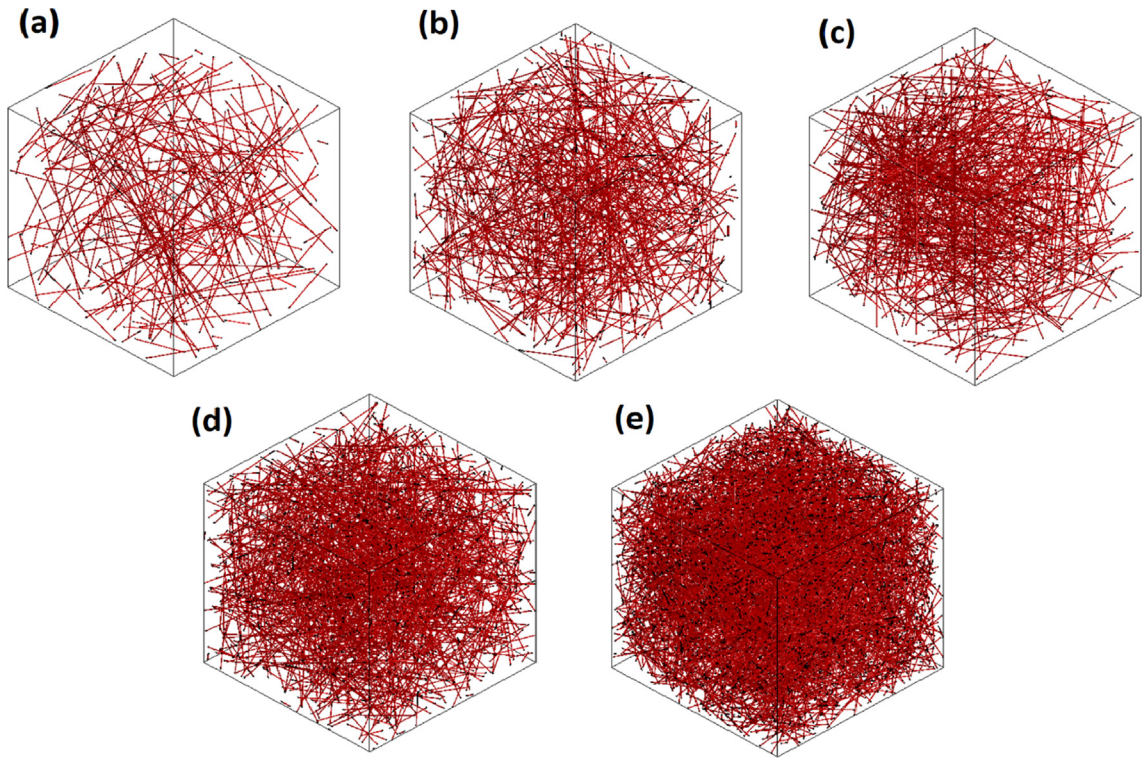

Fig. 1. Generation of RVE with different percentage of MWCNT (a) 0.5 wt%, (b) 1 wt%, (c) 2 wt%, (d) 4 wt%, (e) 5 wt%.

Table 1
Properties of the constituents.

	Epoxy EPON 862	MWCNT
Density (g/cm^3)	1.21	2.1
Young's modulus (MPa)	1650	50,000
Poisson's ratio	0.3	0.261

before the pristine epoxy. Also, the rubber state seems to start at 65 °C, where higher values are presented. Comparing the temperature region of the rubber state from 70 °C to 115 °C of the epoxy sample against the 1 wt% and 2 wt% the storage value incremented steadily from 350 MPa, 450 MPa to 675 MPa respectively. These values reach a steady range. The values of loss modulus in Fig. 4 b) for the glass and rubber state are small and mostly remain constant. However, the values on the glass state are larger. The maxi-

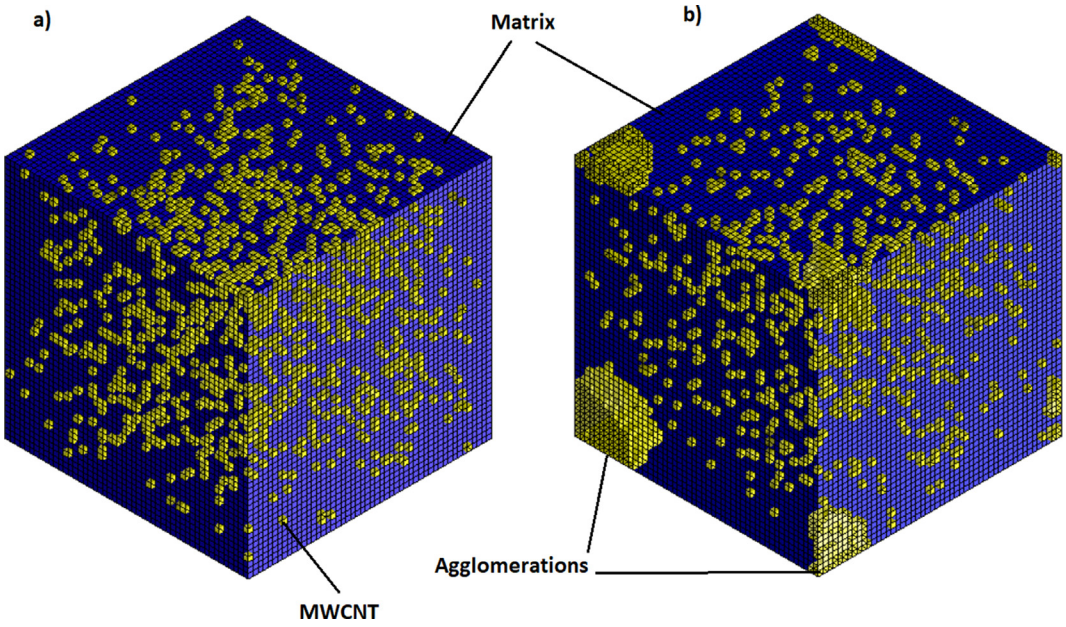

Fig. 2. RVE mesh within the software Digimat a) matrix + MWCNT b) matrix + MWCNT agglomeration.

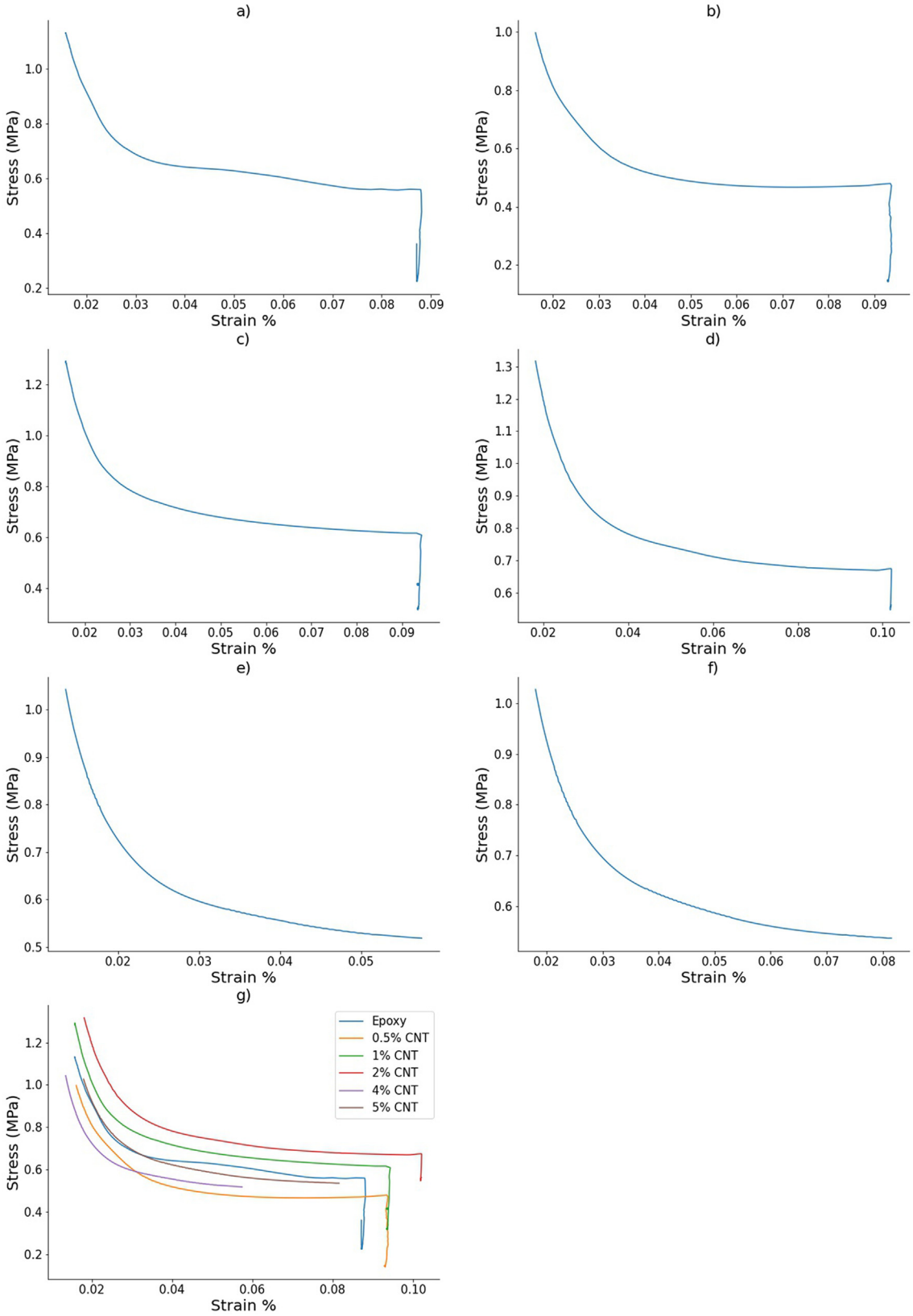

Fig. 3. Stress-strain experimental data temperature dependent a) epoxy b) 0.5 wt%, (c) 1 wt%, (d) 2 wt%, (e) 4 wt%, (f) 5 wt% (g) comparison.

mum value for every sample is attained at the limit of the glass state region, thereafter presenting an abrupt decrement. Fig. 4 c) portraits a similar phenomenon for the loss factor.

The numerical values of the temperature-dependent viscoelastic behaviour are presented in Fig. 5. The simulated storage modulus is shown in blue lines and compared with the experimental

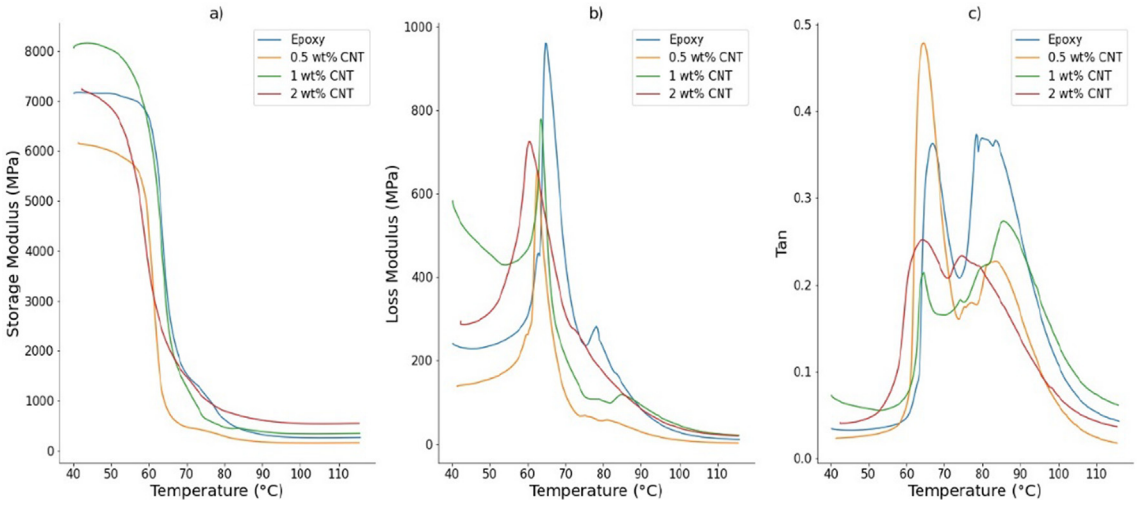

Fig. 4. Experimental results 0.5, 1, 2 wt% CNT: (a) storage modulus; (b) loss modulus; (c) loss factor.

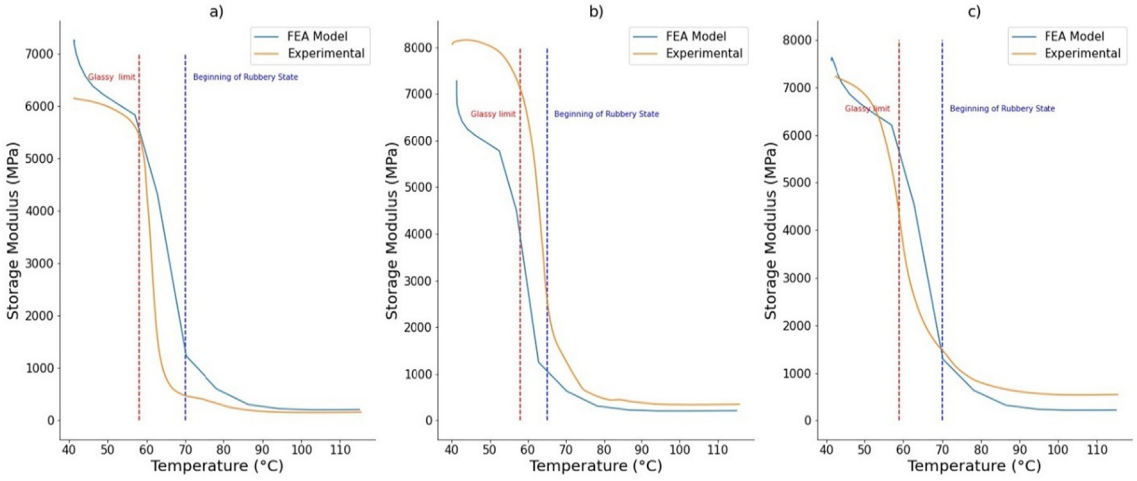

Fig. 5. Modelling vs experimental results: (a) 0.5 wt% MWCNT; (b) 1 wt% MWCNT; (c) 2 wt% MWCNT.

values in orange colour. The numerical models presented in Fig. 5 4 a), b) and c) are capable to predict the behaviour of the samples. The glass, transition and rubber states are clearly distinguished with temperatures obtained in the experimental data. In the glass state, the models do not remain constant as opposed to the experiments, as the temperature transitions in the DIGIMAT software are more influential in the final value of the storage modulus. For instance in Fig. 5. a) the maximum value is presented at the temperature of 40 °C, however, the numerical value is higher by 800 MPa. This value seems to reach a steady and close value of 600 MPa compared with the experimental. The same phenom is presented for the samples 1 wt% and 2 wt% shown in Fig. 5. a) and b) respectively. The difference in the former is only 500 MPa of the experimental value. Nevertheless, the value in the edge of the glass transition presented a difference of 2000 MPa. The models present a good agreement with the experimental data, showing the exact abrupt and short transition temperature regions to the rubber state. In the rubber state, the FEA models are more accurate. The lowest storage values are found from the temperatures ranging from 70 °C to 90 °C, clearly showing the beginning of the rubber state for all samples.

The discrepancy in certain regions in the glass, transition and rubber state is due to a small percentage of nanofillers the attainable properties calculated from the numerical simulations underestimate the intrinsic properties of the carbon nanotubes. Also, at lower percentage of CNT, the meshing is slightly more inaccurate product of the DIGIMAT meshing tools. Additionally, the methods of fabrication, the randomness of distribution and the experimental procedure (i.e. calibration, manipulation, etc.) affect the accuracy of the models. However, this discrepancy seems to be almost negligible with the sample 2 wt% depicted in Fig. 5 c). The model is capable to follow almost an identical profile of the viscoelastic behaviour. One of the reasons is that the higher the percentage the more influence is portrayed in the numerical results. The model predicts the highest value in the glass state with a small difference of 100 MPa. Also, the variance of the storage modulus value along the glass temperature region is highly predicted. A small difference is presented in the transition temperature of 5 °C presenting a discrepancy of 400 MPa. However, the transition state is well predicted. Similarly, the rubber state from both data starts close to 75 °C, where the storage modulus reaches the lowest values and remains constant.

3.2. Effect of MWCNT and agglomerates on the viscoelastic properties

The viscoelastic properties are also affected by the addition of higher quantities of carbon nanotubes. At a higher percentage of carbon nanotubes, the formation of agglomerate/agglomeration is

inevitable. Although these formations can be positive for the electrical properties, the mechanical and especially the viscoelasticity properties are negatively affected [20]. Thus, in Fig. 6 the experimental results of storage modulus (E'), loss modulus (E'') and loss factor (Tan) of the pristine epoxy resin and epoxy/CNT composites are compared with the percentages of 4 and 5 wt% plotted against temperature. The experimental data shows an abrupt change in the temperature regions of the glass, transition and rubber state for the samples containing a high percentage.

For instance, Fig. 6 a) shows the storage values of the two composite samples. The glass transition region seems to be affected and the final temperature is delayed to 95 °C compared to 65 °C of the pristine epoxy sample. This large addition of CNT increments the region where the highest values are obtained. However, the 5 wt% sample showed a quite small value. The highest is only 5600 MPA compared to the pristine epoxy of 7200 MPa. The transition region does not follow a quick transition and it is delayed until 110 °C where the rubber state should begin. The rubber state for these samples are not clearly represented and do not show the constant expected values seen in the pristine epoxy and the samples containing a small percentage of nanofillers i.e. 0.5, 1, and 2 wt%.

The loss modulus (E'') and loss factor (Tan) are also highly affected at this stage of nanofiller addition. For instance, Fig. 6 b) depicting the loss modulus, shows steady and small values in the glass state and rubber state. As opposed to small addition wherein these two different regions higher values were found in the glass state. Also, the highest value is only seen at the peak of the curve where the glass state finishes are smaller compared with the pristine epoxy. The highest value for 4 wt% and % wt% is only 550 MPa and 400 MPa compared with almost 1000 MPa of the Pristine epoxy. A similar phenomenon is seen in Fig. 6 c).

The modelling of the higher percentage of carbon nanotubes was performed using the RVE depict in Fig. 2 b). In this region, the agglomerates are simulated as big bundles of CNTs. As the agglomerates origins, they also create porosity around the nanofillers [20]. This porosity along with the expected porosity from the composite manufacturing process is taken into account for the numerical models.

The numerical values for the temperature-dependent properties are presented in Fig. 7. The models with and without agglomerates are compared with the experimental values shown in the orange profile. Fig. 7. a) and Fig. 7. b) shows the behaviour of the models of 4 wt% and 5 wt% respectively. The model with no agglomerates fails to predict the behaviour of the glass, transition and rubber state. The small region of glass state and transition state behaves as the models containing less percentage of CNT. Also, reach a plateau at the rubber state.

The addition of agglomerates as shown in Fig. 2. b) gives the model a high accuracy. The models with agglomerates are portrayed in the green line. For instance, the 4 wt% model for the glass state region follows the same region limits as the experimental from 40 °C to 85 °C. The high values are within the region of 7000–800 MPa for experimental and modelling with agglomerates. The transition state also is highly predicted by the model showing a slightly more abrupt transition to the rubber state. In this rubber state, the experimental data does not show constants values shown in the modelling and the experimental for less percentage of additives. However, the model is capable of clearly predicting the temperatures of transition of the various states of the sample. Fig. 7. b) displays a similar effect, where the modelling with no agglomerates poorly predicts the behaviour of the sample. On the contrary, the addition of agglomerates in the numerical modelling grant a better performance on the predicted behaviour.

The transition temperatures and regions are clearly predicted by the model, however, there are small discrepancies between the maximum storage modulus within these regions. Due to the nature of agglomerations, and the posterior formation of the porosity around these areas, the discrepancy of the model, at higher percentages of additives, augments. These malformations are unpredictable, in their geometry, ubication and influences. Thus, more difficult to model. The model can be further developed taking into account the interphase properties, the non-uniform distribution of aspect ratios of MWCNT. Also, Different size of RVE could be investigated to obtain a better understanding of the models and the capabilities of predicting the properties below and after the formation of agglomerates.

Also, it seems that the data of experimental and modelling the variation of storage and loss modulus at higher and lower temperatures behave different. In the former temperatures, the storage and loss modulus seems to not vary and reach a plateau, which is expect and known as the rubber plateau, where the molecules and chains of the polymer are stable in this region. On the other hand, at lower temperatures, where the increment and the reaction seem to behave more chaotic for all samples. However this is expected as the steady increment of the temperature starts to alter

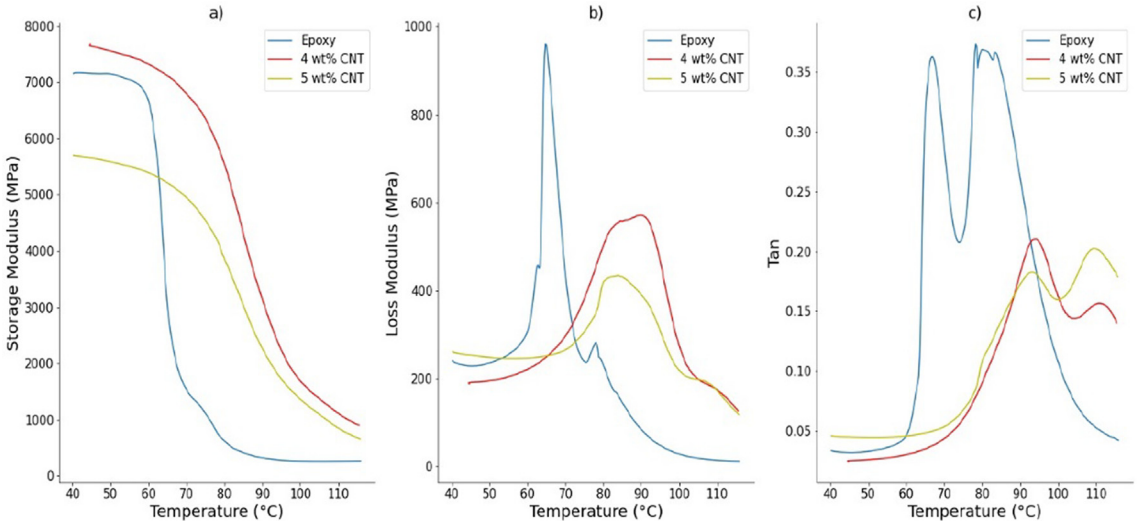

Fig. 6. Experimental results 4, 5 wt% CNT: (a) storage modulus; (b) loss modulus; (c) loss factor.

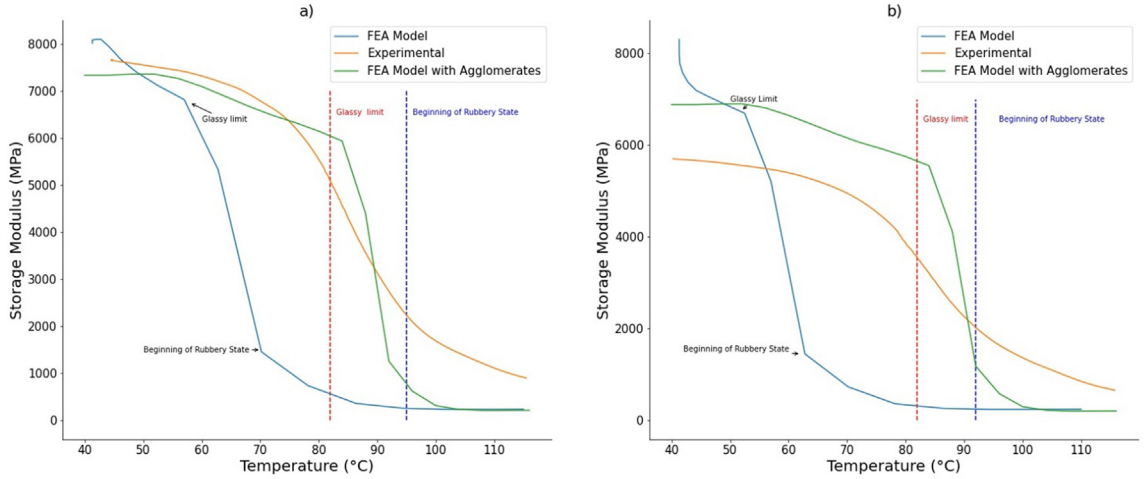

Fig. 7. Modelling vs experimental results: (a) 4 wt% MWCNT; (b) 5 wt% MWCNT.

the molecules and chains of the polymer which until the plateau varies in several points, where the CNT just alter the attainable storage and loss modulus.

4. Conclusions

The temperature-dependent mechanical properties of various CNT/polymer nanocomposites was investigated. Two RVEs models were developed to predict the behavior of the samples containing 0.5, 1, 2, 4, 5 wt%. of MWCNT. The numerical results were compared with the experimental data obtained from the three-bending point method using DMA analysis. The first model was capable to predict the behavior of the samples until the percentage of 2 wt%. Beyond this percentage the formation of agglomerates had occurred, thus affecting the behavior of the samples. A second model was introduced taking into account the agglomeration and the porosity generated in the manufacturing process and within CNT bundles. Both RVEs were highly capable to predict the behavior of the samples. The glass, transition and rubber states regions were clearly calculated in the models. The data suggests that the maximum storage modulus is obtained in the glass state and remains constant until the transition limit. The models were capable to predict the glass transition limit. Also, the abrupt transition region was predicted by the two models, However, with the addition of 4% and 5 wt% the transition and regions temperatures are delayed, showing a more slow transition. The rubber state seems to be the region were the lowest values are found. Comparing the pristine sample with the 0.5%, 1% and 2% the values seem to go through a slight increment confirmed in the experimental data. The samples containing 4 and 5 wt% show a small rubber sate region where the modelling was only capable to predict the temperature transitions. A future investigation is proposed where the experimental procedure should be with different oscillation frequencies. Different dimension of RVE will be investigated for the different frequencies. Finally, the models show good agreement with the experimental data specially on the transitions temperatures of the various states.

CRediT authorship contribution statement

S. Tamayo-Vegas: Writing – original draft, Investigation, Formal analysis, Software, Investigation. **K. Lafdi:** Supervision, Project administration, Validation, Conceptualization, Methodology, Formal analysis, Investigation.

Declaration of Competing Interest

The authors declare that they have no known competing financial interests or personal relationships that could have appeared to influence the work reported in this paper.

Acknowledgment

The authors are grateful to Dr. Ali Muhsan for the samples fabrication and DMA measurements.

References

[1] S. Iijima, Nat. 354 (1991) 56–58.
[2] P.M. Ajayan, O. Stephan, C. Colliex, D. Trauth, Sci. 265 (1994) 1212–1214.
[3] M. Moniruzzaman, K.I. Winey, Mac. 39 (2006) 5194–5205.
[4] F. Du, R.C. Scogna, W. Zhou, S. Brand, J.E. Fischer, K.I. Winey, Mac. 37 (2004) 9048–9055.
[5] F.H. Gojny, M.H.G. Wichmann, U. Köpke, B. Fiedler, K. Schulte, Compos. Sci. Technol. 64 (2004) 2363–2371.
[6] M. Rahmat, P. Hubert, Compos. Sci. Technol. 72 (2011) 72–84.
[7] Z. Spitalsky, D. Tasis, K. Papagelis, C. Galiotis, Prog. Polym. Sci. 35 (2010) 357–401.
[8] F. Zahedi, J. Yao, H. Huang, Smart Mater. Struct. 24 (2015).
[9] S. Gong, Z.H. Zhu, S.A. Meguid, Polymer (Guildf). 55 (2014) 5488–5499.
[10] Q.S. Yang, X.Q. He, X. Liu, F.F. Leng, Y.W. Mai, Compos. Part B Eng. 43 (2012) 33–38.
[11] A. El Moumen, M. Tarfaoui, H. Benyahia, K. Lafdi, J. Compos. Mater. 53 (2019) 925–940.
[12] B. Ashrafi, P. Hubert, S. Vengallatore, Nanotech. 17 (2006) 4895–4903.
[13] M. Tarfaoui, A. El Moumen, K. Lafdi, O.H. Hassoon, M. Nachtane, J. Compos. Mater. 52 (2018) 3655–3667.
[14] A. Montazeri, A. Khavandi, J. Javadpour, A. Tcharkhtchi, Mater. Des. 31 (2010) 3383–3388.
[15] A. Kausar, I. Rafique, B. Muhammad, Polym. - Plast. Technol. Eng. 55 (2016) 1167–2119.
[16] Manoj Kumar Shukla, Kamal Sharma, Polym. Sci. - Ser. A. 61 (2019) 439–460.
[17] R. Ansari, M.K. Hassanzadeh Aghdam, Compos. Part B Eng. 90 (2016) 512–522.
[18] C. Liu, Q. Fang, K. Lafdi, Compos. Commun. 22 (2020) 10051.
[19] M.K. Hassanzadeh-Aghdam, M.J. Mahmoodi, R. Ansari, Compos. Part B Eng. 168 (2018) 274–281.
[20] S. Tamayo-Vegas, A. Muhsan, L. Chang, M. Tarfaoui, K. Lafdi, Mater. Today Proc. (2021).
[21] N. Hu, Z. Masuda, C. Yan, G. Yamamoto, H. Fukunaga, T. Hashida, Nanotech 19 (2008).
[22] M. Mohiuddin, S.V. Hoa, Compos. Sci. Technol. 79 (2013) 42–48.
[23] W. Bauhofer, J.Z. Kovacs, Compos. Sci. Technol. 69 (2009) 1486–1498.
[24] J.Z. Kovacs, B.S. Velagala, K. Schulte, W. Bauhofer, Compos. Sci. Technol. 67 (2007) 922–928.
[25] A. Poorsolhjouy, M.H. Naei, J. Reinf. Plast. Compos. (2015).
[26] Y. Zare, K.Y. Rhee, Compos. Sci. Technol. 144 (2017) 18–25.
[27] A.R. Alian, S. El-Borgi, S.A. Meguid, Comput. Mater. Sci. 117 (2016) 195–220.
[28] M. A. Maghsoudlou, R. Barbaz Isfahani, S. Saber-Samandari, M. Sadighi, Compos. Part B Eng. 175 (2019) 107119.
[29] J. Doh, J. Lee, Comput. Struct. 169 (2016) 91–100.
[30] A. Balakrishnan, M.C. Saha, Mater. Sci. Eng. 528 (2011) 906–913.

[31] G. Gkikas, N.M. Barkoula, A.S. Paipetis, Compos. Part B Eng. 43 (2012) 2697–2705.
[32] E.M. Jackson, P.E. Laibinis, W.E. Collins, A. Ueda, C.D. Wingard, B. Penn, Compos. Part B Eng. 89 (2016) 362–373.
[33] P. Najmi, N. Keshmiri, M. Ramezanzadeh, B. Ramezanzadeh, J. Taiwan Inst. Chem. Eng. 119 (2021) 245–258.
[34] N. Yuca, N. Karatepe, F. Yakuphanoglu, Y.H. Gürsel, Acta Phys. Pol. 123 (2013) 352–354.
[35] B. Arash, W. Exner, R. Rolfes, Comput. Methods Appl. Mech. Eng. 381 (2021) 113821.
[36] V.G. Martynenko, G.I. Lvov, J. Reinf. Plast. Compos. 36 (2017) 1790–2180.
[37] D.K. Rathore, R.K. Prusty, D.S. Kumar, B.C. Ray, Compos. Part A Appl. Sci. Manuf. 84 (2016) 364–376.
[38] F. Bédoui, M. Guigon, Polymer (Guildf). 51 (2010) 5229–5235, 2010,
[39] A.R. Shajari, R. Ghajar, M.M. Shokrieh, Comput. Mater. Sci. 142 (2018) 395–409.
[40] R. Ghajar, M.M. Shokrieh, A.L.I.R. Shajari, Amirkabir. J. Mech. Eng. 48 (2017) 363–370.
[41] Y. Zare, K. Yop Rhee, Res. Phys. 9 (2020) 103537.
[42] J. Feng, Z. Guo, Compos. Part B Eng. 85 (2016) 161–169.
[43] H. Li, B. Zhang, Int. J. Plast. 65 (2015) 22–32.
[44] M. Loos, Carbon Nanotube Reinforced Composites, First Edit., vol. 3. Oxford: William Andrew, 2015.
[45] A. El Moumen, M. Tarfaoui, K. Lafdi, Compos. Part B Eng. 114 (2017) 1–7.